# Monte Carlo simulation of PET images for injection dose optimization

Jiří Boldyš & Jiří Dvořák
*Institute of Information Theory and Automation of the ASCR, Prague, Czech Republic*
Otakar Bělohlávek & Magdaléna Skopalová
*Na Homolce Hospital, PET Center, Prague, Czech Republic*

When a patient is examined by positron emission tomography, radiotracer dose amount has to be determined. However, the rules used nowadays do not correspond with practical experience. Slim patients are given unnecessary amount of radiotracer and obese patients would need more activity to produce images of sufficient quality. We have built a model of a particular PET scanner and approximated human trunk, which is our region of interest, by a cylindrical model with segments of liver, outer adipose tissue and the rest. We have performed Monte Carlo simulations of PET imaging using the GATE simulation package. Under reasonably simplifying assumptions and for special parameters, we have developed curves, which recommend amount of injected activity based on body parameters to give PET images of constant quality. The dependence qualitatively differs from the rules used in clinical practice nowadays and the results indicate potential for improvement.
Keywords: positron emission tomography, Monte Carlo simulation, biological system modeling, image quality

## 1 INTRODUCTION

Positron emission tomography (PET) is a functional imaging modality. Resulting images do not show anatomical objects. They rather display functional processes in a patient body, e.g. glucose metabolism or blood flow. These examinations allow us to monitor tumor treatment, examine epilepsy seizure foci, etc. For a detailed discussion on PET see e.g. Powsner & Powsner (2007).

PET imaging is based on injecting radioactive tracer. For small activities, resulting image quality grows with injected activity amount. However, the dose amount recommendation used nowadays (see Jacobs et al. (2005)) does not sufficiently normalize for image quality in daily routine. Slim patients are given unnecessary amount of radiotracer and obese patients would need more activity to produce images of sufficient quality. Fig. 1 shows examples of CT and PET images of slim and obese patients.

Previous studies published in literature aimed at achieving maximum quality of the resulting image for each patient. This approach might lead to unnecessary radiation exposure of light patients, especially children. A brief overview of these studies, together with different metrics of image quality they use, is presented in Section 2.

The goal of this paper is different – to qualitatively determine, based on significant patient body parameters, the amount of injected radiotracer needed to achieve constant quality of the resulting PET images, even for patients with different body habitus. This would help improve consistency of the diagnostic process.

This paper describes first results of our initial study in this direction. At the beginning of our research, we have adopted several justifiable simplifications explained further on. We limit ourselves to examination of liver and body segment surrounding it.

To achieve our objectives, we have performed Monte Carlo simulations of PET imaging using GATE simulation package. Details, including description of PET scanner and body model, will follow in relevant sections. We will also explain the adopted image quality measure. Finally we come to the desired curves which we call curves of constant quality.

## 2 MAXIMIZING IMAGE QUALITY

Previous studies concerning the dependence of image quality on the amount of the injected radiotracer aimed at maximizing the image quality for each patient. This section provides a brief (and certainly not complete) overview of these studies.

A popular tool for describing quality of PET images is the noise equivalent count, NEC (see Section 7). It quantifies the statistical quality of the raw data and is not affected by the choice of reconstruc-

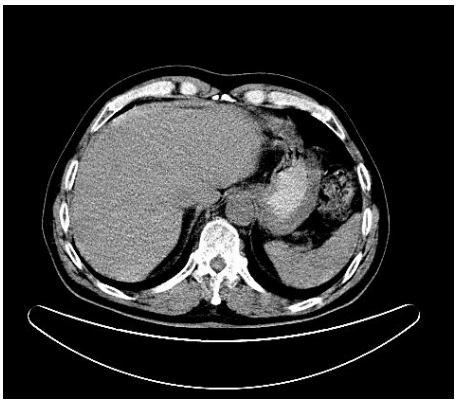

(a) CT - slim patient

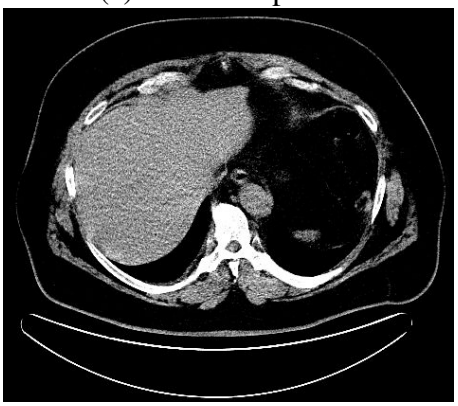

(b) CT - obese patient

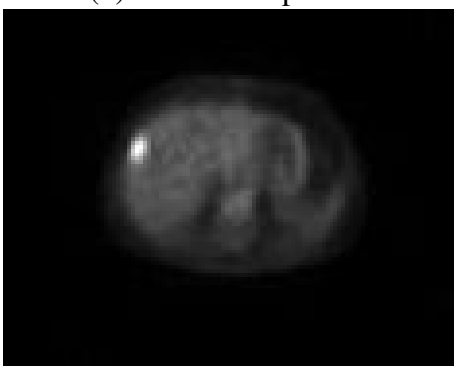

(c) PET - slim patient

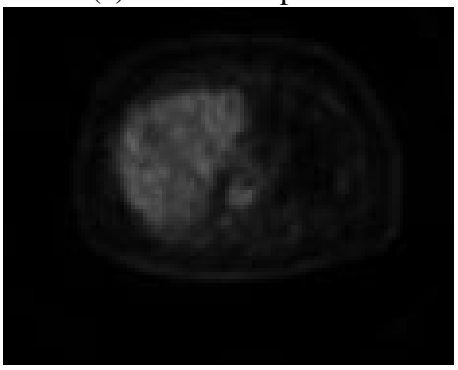

(d) PET - obese patient

Figure 1: CT images of similar transverse plane containing liver - gray homogeneous region on the left. Reader can observe different thickness of the subcutaneous adipose tissue for a slim (a) and an obese (b) patient. Images (c) and (d), resp., show corresponding sections of PET images. Notice lower intensity of the (d) image.

tion algorithm. Studies using NEC to describe PET image quality or modeling the dependence of NEC on the amount of injected activity include Accorsi et al. (2010), Danna et al. (2006), Mizuta et al. (2009) and Watson et al. (2005).

Quality of reconstructed images can be expressed e.g. in terms of signal-to-noise ratio. Relevant references include Mizuta et al. (2009) and Watson (2004).

Other possibility is to assess the subjective visual quality of the images using a numeric scale or verbal description (rating the quality e.g. from excellent to non-diagnostic). This type of psychophysical measurement is usually very time-consuming since the set of analyzed images has to be assessed by one or more experienced practitioners. See e.g. Everaert et al. (2003) or Halpern et al. (2005).

The ultimate measure of PET image quality, from the medical point of view, is performance of a human observer in a given diagnostic task. The most common task is the detection of small foci of increased activity indicating the presence of a tumour. Again, human observer studies are time-consuming and so mathematical model observers were developed to mimic the performance of human observers in a specific task. The most important of these observers are Hotelling and channelized Hotelling observer and their variants. Relevant references include Abbey & Barrett (2001), Gifford et al. (2000) and Halpern et al. (2005).

## 3 RADIOTRACER DOSE IN PET IMAGING

PET examination is useful for example for tumor imaging. Tumors accumulate glucose more than surrounding tissues. Therefore, patient is in advance injected a dose of $^{18}$F-FDG, what is radioactive analogue of glucose. $^{18}$F-FDG is accumulated into tumor and it is emitting positrons. Positrons almost immediately annihilate, resulting into two photons moving in opposite directions and detected approx. at the same time. Reconstructed image is based on number of detected photon pairs and their lines of response (LORs – lines joining two detector segments which detected the photons in coincidence) – see Fig. 2 presenting PET scanner scheme.

There are rules what amount of activity $A$ should be injected into patient. $A$ depends on patient's weight. More weight means more fat, less probability to detect incidences of photon pairs and finally image of worse quality.

It has already been mentioned that todays rules prescribe too much activity to slim patients and insufficient activity to obese patients. There is historical justification for these rules, but everyday clinical practice calls rather for different approach. It would be desirable to produce the same image quality for patients with different body parameters. It is our objective to find prescription for this activity.

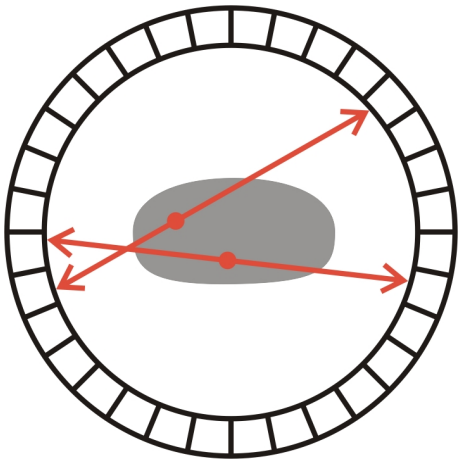

Figure 2: PET modality scheme showing the detector ring, annihilation events (dots) and pairs of photons moving in opposite directions (with their respective LORs).

PET scanner detectors register not only true coincidences, where the photons travel from the annihilation point to the detectors without any interaction. It also happens that photons interact with the tissue and deflect. More tissue causes more photon deflections and finally wrong LOR attributions - they are called scattered coincidences. Furthermore, so called random coincidences happen when two photons from two different annihilations are detected at the same time.

Scattered and random coincidences have undesired effect on the resulting image. They introduce blurring and noise to the data.

Numbers of all coincidences grow with increasing activity. However, random coincidence count grows the fastest, causing image quality to deteriorate above some injected activity. This means that for obese patients with high amounts of injected activity we might not be able to get image of sufficient quality.

## 4 MONTE CARLO SIMULATIONS

Process of PET imaging can be modeled by Monte Carlo methods. There are several simulation packages available for this purpose. We have chosen the GATE simulation package, see Jan et al. (2004). GATE is an open-source software and currently it is able to simulate PET, SPECT and CT imaging. GATE is developed by OpenGATE collaboration.

The main GATE component is the Geant4 toolkit for the simulation of the passage of particles through matter. It allows us to model usual particle physics interactions, like Compton or Rayleigh scattering, etc.

GATE performs PET imaging simulation after specifying the following: PET scanner model, phantom model (in our case body model), source model, time of examination, and eventually other data. In the next sections body and scanner models are commented in detail.

## 5 PATIENT MODEL

For general PET imaging simulations, an elaborate full body model would find its use. Our first objectives are rather qualitative and thus we can afford a very simplified body model at this stage. In this paper we choose liver as our main region of interest. Thus we confine ourselves to the trunk area surrounding liver with some overlap.

We further attempt to simplify model of a transverse section through a body in liver area from the point of view of PET imaging. We segment the section into three areas: subcutaneous adipose tissue SA (underskin fat), liver LI, and everything inside SA, what we call inner segment IS, see Fig. 3. We have a database of 18 CT images, where we have localized one reference transverse section based on liver shape. The three defined segments were then manually segmented and areas of segments SA and IS were measured. These areas were then recalculated into effective radii $R_{SA}$ and $R_{IS}$ of corresponding cylinder bases.

On our limited set of CT images, radii $R_{SA}$ and $R_{IS}$ can be statistically explained using linear regression by patient's weight $m$ and height $h$ only. Other parameters such as age or BMI were found insignificant (in statistical sense). We initially focus only on male patients due to different way of fat deposition. To further simplify the simulations we set $h$ = 180 cm and we vary only the weight $m$.

Cylindrical model of patient's trunk is then constructed as follows, see Fig. 3(b). Cylinder with height 25 cm and radius $R_{IS}$ models the inner segment. It is surrounded by another cylindrical layer with radius $R_{SA}$ which models the SA segment. Liver is modeled by a sphere with radius $R_{IS}/2$ touching the far left point of the IS segment. The radii $R_{SA}$ and $R_{IS}$ depend on the parameter $m$ and are determined according to the linear regression model mentioned above.

Materials for all the segments were appropriately chosen from the GATE material database. As for the distribution of activity in the model of patient's trunk, we chose homogeneous distribution in all the segments SA, LI and IS. The ratios of unit activity (activity per cubic centimeter) in different segments correspond to average ratios determined from PET images of real patients. Such kind of a simple model filled with specified materials was found sufficient to approximate body region of interest for PET imaging simulations.

## 6 SCANNER MODEL

Siemens Biograph40 TruePoint TrueV HD PET scanner is modeled in this contribution. It is a cylindrical type of scanner, see Fig. 4. Necessary technical data were kindly provided by technicians of both the PET Center of Na Homolce Hospital in Prague and

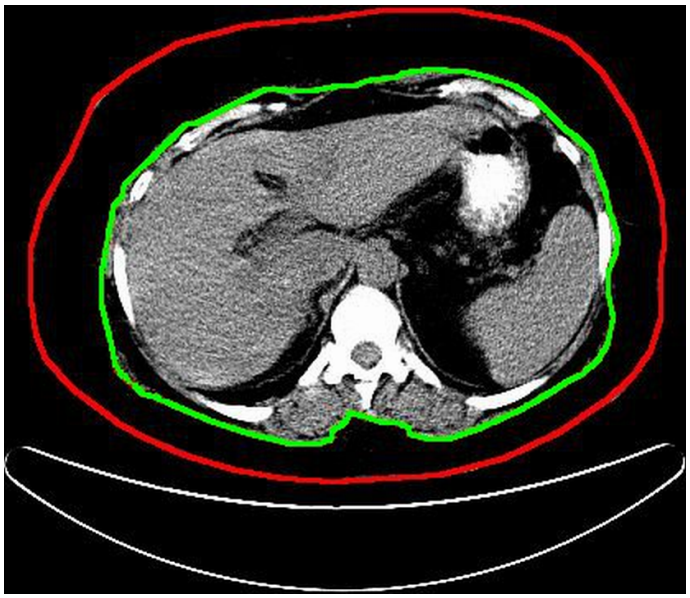

(a) Segmentation of SA and IS

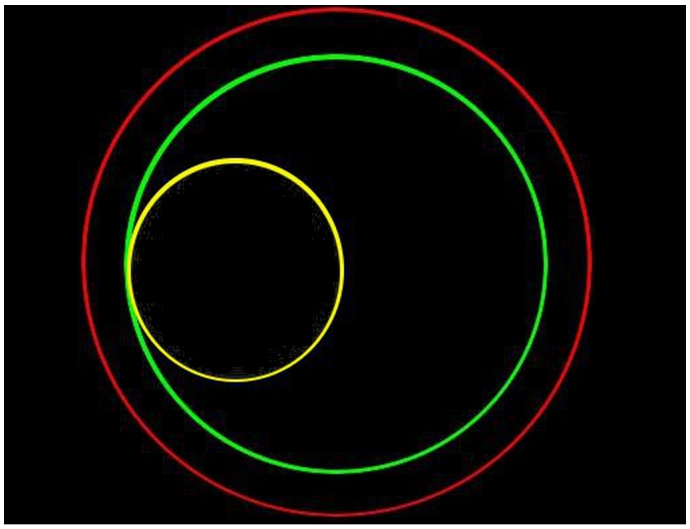

(b) Cylindrical body model

Figure 3: (a) CT images were segmented to get the SA and IS segments. Their areas are basis of the equivalent cylindrical model (b).

Siemens company. Simulated acquisition time was 60 s.

## 7 IMAGE QUALITY ASSESSMENT

There are many image quality measures available in the field of image analysis. Overview of such measures suitable for PET imaging was given in Section 2. For the purpose of this paper so called noise equivalent count (NEC) was chosen. It is a very simple and right sufficient measure for our objectives. At the same time it is widely used in nuclear medicine community. Moreover, it is not affected by the choice of reconstruction algorithm, so in fact no reconstruction was needed for this study.

It is based on the total numbers of true coincidences $T$, scattered coincidences $S$ and random coincidences $R$. Data for NEC calculation are available from outputs of our simulations and there is no need for tomographic reconstruction.

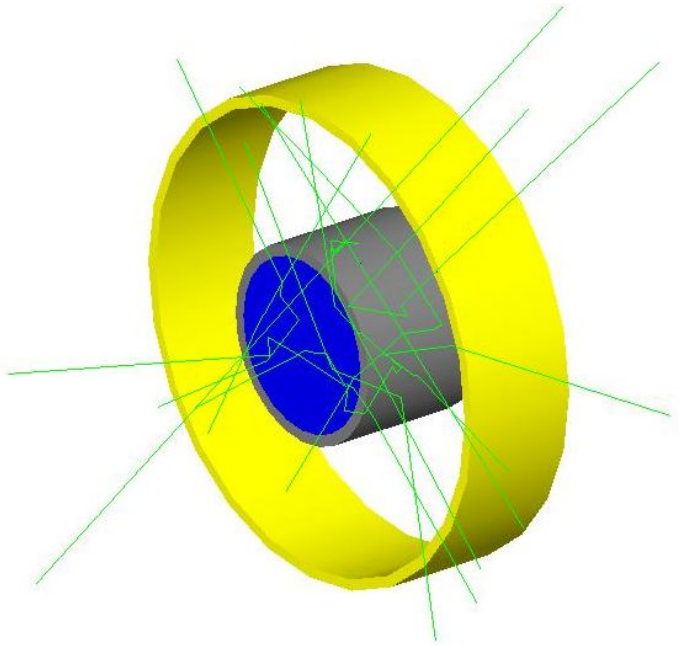

(a) Detector ring, body model

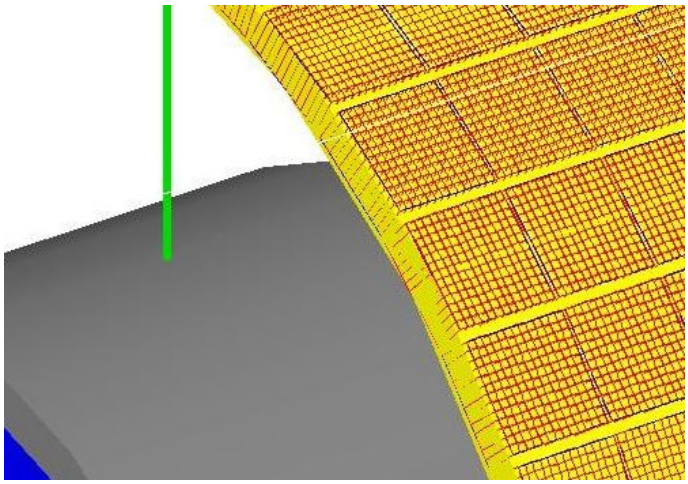

(b) Detector crystals - closeup

Figure 4: Model of our studied PET scanner together with the body region of interest used in GATE simulations. (a) – the whole setup, (b) – closeup. In the body model, adipose tissue and the inner segment are visible. Liver is hidden inside and it is not visible.

$$\text{NEC} = \frac{T^2}{T + S + R}$$

NEC equals $T$ times the ratio of true coincidences to the number of all coincidences. Thus it can be intuitively interpreted as an effective number of true coincidences with respect to the resulting image quality. Due to behavior of dependences of $T$, $S$ and $R$ on activity $A$ mentioned earlier in this paper, dependence NEC$(A)$ is first growing and then decreasing.

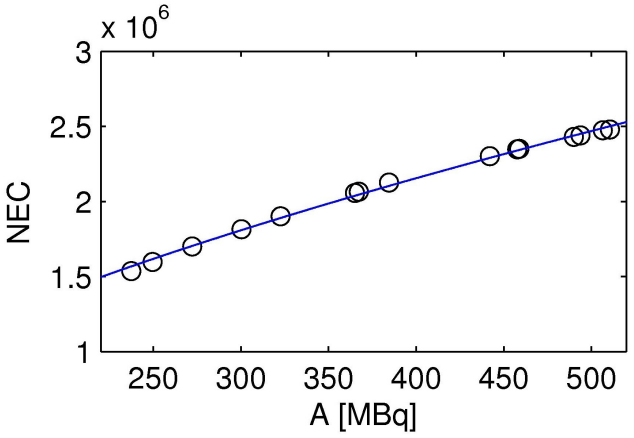


Figure 5: Dependence of NEC image quality measure on simulated activity for a particular patient model ($m$ = 81 kg).

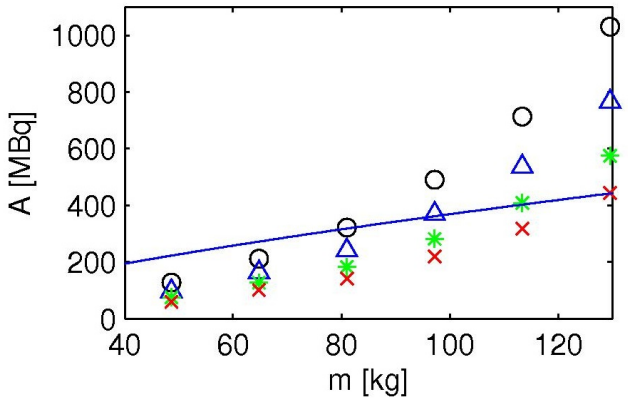


Figure 6: Prescription for applied activity based on patient weight. Different symbols correspond to different reference image quality NEC. For example, circles determine the amount of activity that would produce images with the same NEC as was achieved in simulation of patient with $m$ = 81 kg. Solid line – activity injected according to the rule currently used in medical practice.

## 8 SIMULATION RESULTS

We have performed PET imaging simulations with the PET scanner model and patient body model described above. For simplicity and as mentioned above, we were varying only the weight parameter $m$. Simulated activities are far covering the range examined in practice.

We simulated 6 different weights evenly distributed in the range from 48 kg to 130 kg. From the given weight and default height 180 cm we calculated parameters $R_{SA}$ and $R_{IS}$ needed to specify the patient body model. For every patient (i.e. for every weight) we performed 15 PET imaging simulations with varying activity. NEC was then computed for every simulation based on $T$, $S$ and $R$. Results for one particular weight are plotted in Fig. 5.

One additional simulation with the activity determined according to Jacobs et al. (2005) was performed to provide a reference level of NEC for the given weight.

Resulting dependence NEC$(A)$ can be fitted by a curve NEC$(A) = p_1 + p_2 A^{p_3}$, where $p_i$'s are fitted parameters. The resulting curve can be used to propose activity $A$, which has to be used to achieve a reference NEC for particular patient weight.

Such activities are plotted in Fig. 6. Different symbols correspond to different levels of reference image quality NEC. Solid line shows the prescription used today in clinical practice.

It is evident that the dependence of injected activity on body parameters is qualitatively different from the prescription used nowadays. The resulting curves of constant quality (interpolated through the marks) show rather convex tendency on the contrary to todays standard.

The results support observations from clinical practice. It seems that there is potential to save slimmer patients from radiation load, what is crucial for reducing the potential risk of radiation induced cancer by PET investigation. On the other hand, we have a methodology how to find suitable activities for simulated obese patients to get clinically informative PET image.

## 9 CONCLUSIONS

In this paper we describe our PET imaging simulations using the GATE package. We provide details about the body region of interest and about the PET scanner. We use the NEC global image quality measure to derive curves of constant quality. We show how image quality depends on injected activity for particular body parameters.

We have achieved the main goal of this study - we have derived curves of constant quality, which qualitatively predict the amount of injected radiotracer to produce resulting PET image of constant quality, for particular body parameters. The results support clinical experience of physicians performing PET examinations. Based on these results, the PET Center of Na Homolce Hospital in Prague has started a clinical study.

Our plans for the future include elaboration of more realistic body model. We will investigate also other image quality measures.

## 10 ACKNOWLEDGMENTS

We are very grateful to Filip Šroubek, Pavel Máca and Radek Matějka for fundamental technical help. Also many thanks to the OpenGATE Collaboration for GATE development.

This work has been supported by the Czech Ministry of Education under the project No. 1M0572 (Research Center DAR).

REFERENCES

[1] Abbey, C.K. & Barrett, H.H. 2001. Human- and Model-Observer Performance in Ramp-Spectrum Noise: Effects of Regularization and Object Variability. *The Journal of the Optical Society of America A* 18 (3): 473–488.

[2] Accorsi, R., Karp, J.S. & Surti, S. 2010. Improved Dose Regimen in Pediatric PET. *The Journal of Nuclear Medicine* 51 (2): 293–300.

[3] Danna, M., Lecchi, M., Bettinardi, V., Gilardi, M.C. & Stearns, C.W. 2005. Generation of the Acquisition-Specific NEC (AS-NEC) Curves to Optimize the Injected Dose in 3D $^{18}$F-FDG Whole Body PET Studies. *IEEE Transactions on Nuclear Science* 53 (1): 86–92.

[4] Everaert, H., Vanhove, C., Lahoutte, T., Muylle, K., Caveliers, V., Bossuyt, A. & Franken P.R. 2003. Optimal Dose of $^{18}$F-FDG Required for Whole-Body PET Using an LSO PET Camera. *European Journal of Nuclear Medicine and Molecular Imaging* 30 (12): 1615–1619.

[5] Gifford, H.C., King, M.A., de Vries, D.J. & Soares, E.J. 2000. Channelized Hotelling and Human Observer Correlation for Lesion Detection in Hepatic SPECT Imaging. *The Journal of Nuclear Medicine* 41 (3): 514–521.

[6] Halpern, B.S., Dahlbom, M., Auerbach, M.A., Schiepers, C., Fueger, B.J., Wolfgang A. Weber, W.A., Daniel H.S. Silverman, D.H.S., Ratib, O. & Czernin, J. 2005. Optimizing Imaging Protocols for Overweight and Obese Patients: A Lutetium Orthosilicate PET/CT Study. *The Journal of Nuclear Medicine* 46 (4): 603–607.

[7] Jacobs, F., Thierens, H., Piepsz, A., Bacher, K., Van de Wiele, C., Ham, H. & Dierckx, R.A. 2005. Optimised tracer-dependent dosage cards to obtain weight-independent effective doses. *European Journal of Nuclear Medicine and Molecular Imaging* 32 (5): 581–588.

[8] Jan, S., Santin, G., Strul, D., Staelens, S., Assie, K., Autret, D., Avner, S., Barbier, R., Bardies, M., Bloomfield, P.M., Brasse, D., Breton, V., Bruyndonckx, P., Buvat, I., Chatziioannou, A.F., Choi, Y., Chung, Y.H., Comtat, C., Donnarieix, D., Ferrer, L., Glick, S.J., Groiselle, C.J., Guez, D., Honore, P.F., Kerhoas-Cavata, S., Kirov, A.S., Kohli, V., Koole, M., Krieguer, M., van der Laan, D.J., Lamare, F., Largeron, G., Lartizien, C., Lazaro, D., Maas, M.C., Maigne, L., Mayet, F., Melot, F., Merheb, C., Pennacchio, E., Perez, J., Pietrzyk, U., Rannou, F.R., Rey, M., Schaart, D.R., Schmidtlein, C.R., Simon, L., Song, T.Y., Vieira, J.M., Visvikis, D., Van de Walle, R., Wieers, E. & Morel, C. 2004. GATE: a simulation toolkit for PET and SPECT. *Physics in Medicine & Biology* 49 (19): 4543–61.

[9] Mizuta, T., Senda, M., Okamura, T., Kitamura, K., Inaoka, Y., Takahashi, M., Matsumoto, K., Abe, M., Shimonishi, Y. & Shiomi, S. 2009. NEC Density and Liver ROI S/N Ration for Image Quality Control of Whole-Body FDG-PET Scans: Comparison with Visual Assessment. *Molecular Imaging and Biology* 11 (6): 480–486.

[10] Powsner, R.A. & Powsner, E.R. 2007. *Essential nuclear medicine physics*. Wiley-Blackwell.

[11] Watson, C.C. 2004. Count Rate Dependence of Local Signal-to-Noise Ratio in Positron Emission Tomography. *IEEE Transactions on Nuclear Science* 51 (5): 2670–2680.

[12] Watson, C.C., Casey, M.E., Bendriem, B., Carney, J.P., Townsend, D.W., Eberl, S., Meikle, S. & DiFilippo, F.P. 2005. Optimizing Injected Dose in Clinical PET by Accurately Modeling the Counting-Rate Response Functions Specific to Individual Patient Scans. *The Journal of Nuclear Medicine* 46 (11): 1825–1834.